Implementation and validation of a hydro – mechanical model based on the Clay and Sand Model extended to unsaturated conditions

Arianna Pucci[1,*], *Ignacio* Giomi[2], *Giulia* Guida[1], *Vicente* Navarro[3] and *Francesca* Casini[1]

[1]Università degli Studi di Roma "Tor Vergata", Dipartimento di Ingegneria Civili e Ingegneria Informatica (DICII),Via del Politecnico 1, 00133, Roma, Italia.
[2]eCampus University, Department of Theoretical and Applied Sciences, Via Isimbardi 10, Novedrate, Italy.
[3]Universidad de Castilla – La Mancha, Geoenviromental Group, Av.da Camilo José Cela, 13071 Ciudad Real, España

Abstract. Wetting -induced collapse settlements are a brittle and irreversible phenomenon that can cause significant structural damage and economic losses. These deformations primarily occur in loose and unsaturated soils triggered by water infiltration due to precipitation, pipe leakage, or a rising water table. Modelling this phenomenon requires a comprehensive hydro-mechanical (H-M) coupling approach to capture the interaction between hydraulic and mechanical processes within the soil. This approach involves the simultaneous solution of the water mass balance and mechanical equilibrium equations. In this study, the commercial software COMSOL Multiphysics® was used as an implementation platform to develop a numerical solver to simulate different laboratory tests, including triaxial tests under constant and variable suction. The Clay and Sand Model (CASM), extended to unsaturated conditions by incorporating Bishop's effective stress and suction as stress variables, called U-CASM, was employed as the constitutive model. The CASM framework provides a unified elastic-plastic model capable of capturing the behaviour of both clayey and sandy soils. The use of symbolic algebra facilitated an efficient implementation, with an integration strategy based on the Current Increment Corrects Error (CICE) method, which reduces potential integration drift. The model was verified against predictions obtained by other numerical tools with the same constitutive model and subsequently calibrated and validated considering experimental results available in literature. The comparison with experimental data demonstrated that the model accurately reproduces the soil behaviour under different suction and loading conditions.

1 Introduction

The partially saturated condition of the soils above the water table is often neglected in practical applications and design. This is largely because suction increases shear strength and stiffness [1,2]. However, from a volumetric perspective, these soils can also exhibit complex and challenging behaviours. When subjected to wetting processes, partially saturated soils may undergo instability, known in the literature as collapse upon saturation. This phenomenon involves the accumulation of compressive plastic strains triggered by saturation, leading to irreversible settlements and in many cases sudden volume reductions [3] .

Saturation-induced collapse can result in severe structural damage. Notable examples include the case of Via Settembrini in Naples, Italy, where heavy rainfall in 2004 caused widespread damage to existing buildings [4]. Similarly, in Pereira Barreto, Brazil, the construction of a dam led to a rising water table, which caused serious damage to nearby structures [5].

One of the earliest advanced constitutive models for partially saturated soils, and capable of capturing the collapse upon saturation phenomenon, is the Barcelona Basic Model (BBM) [1]. As an extension of the Modified Cam-Clay model [6], BBM better reproduces the behaviour of clays than sands It employs net stress ($\sigma_n = \sigma - u_a$) and suction ($s = u_a - u_w$) as stress variables.

The BBM presents some limitations arising from its choice of stress state variables. For instance, it does not explicitly account for the dependence of the degree of saturation on suction, and it does not naturally reduce to Terzaghi's effective stress under saturated conditions.

This study presents an extension of the Clay and Sand Model (CASM, [7]) to the unsaturated conditions. The extension of CASM, called U-CASM, uses Bishop's effective stress [8] and suction as stress variables, trying to overcome the limitations mentioned above for the BBM. The U-CASM is then implemented in a straightforward and versatile manner in the commercial finite element software, COMSOL Multiphysics, taking advantages of its symbolic algebra capabilities.

* Corresponding author: arianna.pucci@uniroma2.it

The U-CASM has been successfully adopted to predict the triggering mechanisms of shallow landslides upon rainfall (e.g. [9]) and it will be used to predict the behaviour observed within the PROmise project [10].

To assess the effectiveness of this implementation, a numerical validation is also presented. Laboratory tests have been simulated using U-CASM, and the results have been compared with those obtained from other implementations of CASM for both saturated and unsaturated conditions, already available in the literature.

2 Clay and Sand model and its extension to unsaturated conditions (U-CASM)

The Clay and Sand Model (CASM) is a hardening elastic-plastic constitutive model based on critical state theory developed by Yu in 1998 [7]. Equation (1) defines the yield surface adopted in the model:

$$f(p', q, p_0') = (q/Mp')^n + \ln(p'/p_0')/\ln(r) \quad (1)$$

where q is the deviatoric stress, p' is the mean effective stress, and p_0' is the preconsolidation pressure. M is the slope of the critical state line, while n and r are dimensionless model parameters that depend on the material. Specifically, n controls the inclination of the yield ellipse, whereas r defines its intersection with the critical state line, as illustrated in Fig. 1.(a) and Fig. 1.(b), respectively.

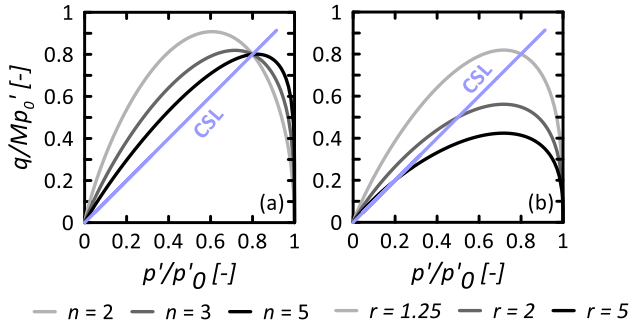

Fig. 1. (a) Effects of the parameter n on the yielding surface and (b) effects of the parameter r on the yielding surface.

CASM adopts a non-associated flow rule, with a plastic potential derived from the integration of Rowe's dilatancy equation [11], given in Equation (2):

$$d = d\varepsilon^p_p / d\varepsilon^p_q = 9(M-\eta) / 9+3M-2M\eta \quad (2)$$

where $d\varepsilon^p_p$ represents the increment of plastic volumetric strains, while $d\varepsilon^p_q$ denotes the increment of plastic deviatoric strains. The parameter η is the stress ratio, defined as q/p'.

Finally, CASM adopts a volumetric hardening law identical to that used in the Modified Cam-Clay model [6], as follows:

$$dp_0' = [(1+e)\cdot p_0' / (\lambda(0) - \kappa)]\, d\varepsilon^p_p \quad (3)$$

where dp_0' describes the increment of preconsolidation pressure, e is the void ratio, $\lambda(0)$ is the slope of the normal consolidation line under saturated conditions in the $v - \ln(p')$ plane, and κ is the slope of the unloading–reloading line in the same plane.

2.1 U-CASM: extension of the Clay and Sand Model to the partially saturated case

The extension of the CASM to unsaturated conditions requires the consideration of the fundamental characteristics of partially saturated soils. These soils are three-phase systems consisting of solid particles, pore water, and pore air. According to the general framework, $i - 1$ independent stress variables are required to fully describe the mechanical behaviour of a system with i phases. Therefore, for unsaturated soils, two stress variables must be employed. These variables are typically formulated from combinations of total stress, pore water pressure, and pore air pressure. In the present work, suction and Bishop's effective stress [8] were adopted as the governing stress variables, as defined in Equations (4) and (5).

$$s = u_a - u_w \quad (4)$$

$$p' = p - u_a + \chi(S_r)(u_a - u_w) \quad (5)$$

where u_a is the pore air pressure, u_w is the pore water pressure and $\chi(S_r)$ is a parameter that depends on the degree of saturation [12,13], equal to 1 in saturated conditions and 0 in dry conditions. Several expressions relating $\chi(S_r)$ and S_r are available in the literature [14-16], but the simplest ways is to consider is $\chi(S_r) = S_r$.

The main advantage of using Bishop's effective stress over net stress as a stress variable lies in its ability to that ensure a continuous transition between saturated and unsaturated conditions, as it reduces to Terzaghi's effective stress in saturated conditions, where $u_a = 0$ and $\chi(S_r) = 1$.

In addition, to consider the effect of the increase of stiffness and strength caused by suction increase, the compressibility index (λ) and the preconsolidation (p_0') pressure can be defined as a function of suction [1], as follows:

$$\lambda(s) = \lambda(0)[(1-r_{LC})\exp(-\beta s) + r_{LC}] \quad (6)$$

$$p_0(s) = p_c(p_0^*/p_c)^{\lambda(0)-\kappa/\lambda(s)-\kappa} \quad (7)$$

where r_{LC}, β and p_c are material parameters, and p_0^* is the preconsolidation pressure in saturated conditions. The relationship between preconsolidation pressure and suction defines an additional yield surface in the p - s plane, known as Loading Collapse [1].

By replacing the Terzaghi effective stress with Bishop's effective stress and expressing the preconsolidation pressure as a function of suction, the yield surface in Equation (1) can be extended to unsaturated condition, as reported below:

$$f(p', q, p_0') = (q/Mp')^n + \ln(p'/p_0'(s))/\ln(r) \quad (8)$$

where $p_0'(s)$ is the preconsolidation pressure in unsaturated conditions expressed in terms of Bishop's effective stress:

$$p_0'(s) = p_0(s) + \chi(S_r)(u_a-u_w) \quad (9)$$

For the coupled hydro-mechanical model was introduced the water retention curve defined by Van Genuchten [17], as reported in Equation (10). Additionally, the relative permeability function k_{rel} was introduced, which describes the reduced permeability of partially saturated soils compared to saturated ones, as a function of S_r, as shown in Equation (11).

$$S_r(s) = S_{r,res} + (S_{r,max} - S_{r,res})[1+(s/P)^{n_{VG}}]^{-m_{VG}} \quad (10)$$

$$k_{rel}(S_r) = S_e^{0.5}[1-(1- S_e^{1/m_{VG}})]^2 \quad (11)$$

where P, n_{VG} and m_{VG} are model parameters, $S_{r,res}$ is the residual degree of saturation, $S_{r,max}$ is the maximum degree of saturation, generally equal to 1, and S_e is the effective degree of saturation, defined as follows:

$$S_e = (S_r - S_{r,res}) /(S_{r,max} - S_{r,res}) \quad (12)$$

3 Hydro – Mechanical coupling and U-CASM implementation

The U-CASM implemented in COMSOL (2021) is intended to solve coupled hydro – mechanical problems. In this preliminary phase, a single-porosity approach was adopted, disregarding the presence of micropores. Furthermore, variations in air and vapor pressure are considered negligible. As a result, the unknowns in the analysis are the vector of the solid skeleton displacements $\boldsymbol{u}$ and the liquid pressure u_w. To determine their values the water mass balance equation and the mechanical equilibrium equation must be solved. Tensors and vectors are all reported in bold.

3.1 Hydro – Mechanical coupling

The water mass balance is given by:

$$[1/(1+e_{TOT})][\partial(\rho_w S_r e_{TOT})/ \partial t]+ \nabla\cdot(\rho_w \boldsymbol{q_L}) = 0 \quad (13)$$

where ρ_w is the water density, e_{TOT} is the void ratio, and $\boldsymbol{q_L}$ represents the water flux, defined by the Darcy's law as follow:

$$\boldsymbol{q_L} = - k_{rel}K_{sat}(\nabla u_w+\rho_w g \nabla z)/ \rho_w g \quad (14)$$

where k_{rel} is the relative permeability introduced in Equation (11), while K_{sat} is the hydraulic conductivity for the soil in saturated conditions.
The mechanical equilibrium equation, on the other hand, is given by:

$$\nabla\cdot\boldsymbol{\sigma} - \boldsymbol{f} = 0 \quad (15)$$

where $\boldsymbol{\sigma}$ is the total stress tensor and $\boldsymbol{f}$ corresponds to the vector of external forces. The total stress tensor can be determined by inverting the definition of Bishop's effective stress reported in Equation (5), as follows:

$$\boldsymbol{\sigma} = \boldsymbol{\sigma'} + \boldsymbol{u}_a - \chi(S_r)(\boldsymbol{u}_a-\boldsymbol{u}_w) \quad (16)$$

where $\boldsymbol{\sigma'}$ is the Bishop's effective stress, referred to as 'Constitutive Stress', because it characterises the mechanical behaviour of the soil and it is used to formulate the constitutive model. Consequently:

$$d\boldsymbol{\sigma'} = \boldsymbol{D}^e d\boldsymbol{\varepsilon}^e \quad (17)$$

where $\boldsymbol{D}^e$ is the elastic matrix, and $d\boldsymbol{\varepsilon}^e$ is the increment of the elastic deformations, which, under the assumption of an additive formulation, can be defined as:

$$d\boldsymbol{\varepsilon}^e = d\boldsymbol{\varepsilon} - d\boldsymbol{\varepsilon}^p \quad (18)$$

where $d\boldsymbol{\varepsilon}$ is the total strains increment and $d\boldsymbol{\varepsilon}^p$ the increment of plastic strains that depends on the plastic model adopted. For the plasticity of unsaturated CASM reference can be made to Navarro et al. [18].

3.2 Implementation of the U-CASM

COMSOL Multiphysics belongs to a class of software known as Multiphysics Partial Differential Equation Solvers (MPDES), where the user defines the governing equations and constitutive formulation, while the software handles the assembly of the system of equations and their numerical solution.

Among the existing MPDES, COMSOL is a very convenient option to solve coupled boundary problems. In particular, this software, based on the application of the finite element method (FEM) with Lagrange multipliers, applies automatic symbolic differentiation techniques to generate a high-quality system iteration matrix, thus improving the model's numerical performance [19-21].

COMSOL Multiphysics provides several built-in modules for solving partial differential equations, such as those governing fluid flow in porous media, which incorporate various predefined laws (e.g., Richard's equation). It also provides some constitutive formulations, already implemented, such as the modified Cam – Clay model for saturated soils and the Barcelona Basic Model for unsaturated conditions. However, in this work, both the mechanical and hydraulic components are solved without relying on these built-in modules, instead following the approach proposed in [21], using COMSOL as an implementation platform. All the parameters and variables can be introduced as text rows, using the Parameters and Variables blocks provided by COMSOL.

3.2.1 Implementation steps

The implementation of the H-M model, depicted in section 3.1, was carried out in seven tasks, as outlined in Fig.2. The first task involves the development of a Parameters Library (PP-L), where the input parameters are reported and remain constant during the simulation.

In the second task, the Hydraulic Library (H-L) was created, in which were reported the terms of the water mass balance equation in Equation (13), the water

retention curve in Equation (11) and the relative hydraulic conductivity in Equation (10).

The Bishop's effective stress, reported in Equation (5), was defined in the third task, named as Mechanical Library (M-L), as well as the deviatoric stress and the total stress.

At the fourth step, the Constitutive Library (C-L) was created, containing the implementation of the constitutive model. To compute the plastic increments, the following components were defined: the yield function in Equation (8), the compression index in Equation (6) and the preconsolidation pressure in Equation (7) - both as a function of suction – along with the Rowe's dilatancy law, reported in Equation (2). The plastic strains increments are then evaluated by applying the consistency condition, as reported in [18]. As mentioned, the automatic symbolic differentiation performed by COMSOL Multiphysics on the expressions contributing to the iteration matrix enhances the computational convergence rate. However, as noted in [20,21], challenges can arise when state functions are defined implicitly, since their symbolic derivatives cannot be computed, leading to issues in defining the iteration matrix. To address this, following the mixed approach proposed in [20], σ' and p_0* can be treated as two additional primary unknowns. Unlike the other variables, $\boldsymbol{u}$ and u_w, which are governed by partial differential equations, these two new unknowns are solved through ordinary differential equations (ODEs), where the time derivatives of σ' and p_0* are respectively defined by Equation (17) and Equation (3) in the C-L. Solving these two ordinary differential equations constitutes the fifth task in Fig. 2, referred to as "ODE's".

In the sixth task, the partial differential equation (PDE) representing the water mass balance (Equation (13)) is implemented, using the general PDE solver interface provided by COMSOL.

The seventh and last task is the one where mechanical equilibrium equation is solved. Applying the variational equilibrium expression provided by the Principle of Virtual Works (PVW), it is verified that the displacements field, $\boldsymbol{u}$, and the total stress, σ, obtained from the local integration of σ' and the general integration of u_w, are statically admissible with the mechanical loads and kinematic constraints imposed to the system.

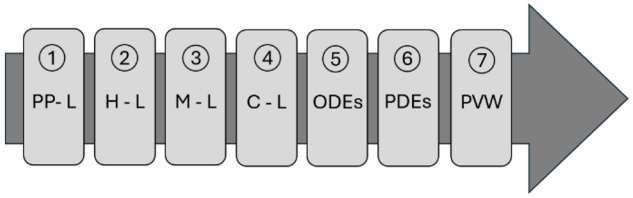

Fig. 2. Tasks performed for the implementation of the extended CASM in COMSOL Multiphysics (after [21])

4 U-CASM numerical validation

To validate the code described in the previous section, several laboratory tests were reproduced. Its performance was then compared with numerical results from other CASM implementations available in the literature. These comparisons involved a wide range of triaxial tests on different materials, including clays and sands, under both saturated and unsaturated conditions.

4.1 Saturated performance of the U-CASM

To demonstrate the effectiveness of the new U-CASM implementation, validation was conducted using a series of saturated triaxial tests. These included both drained and undrained conditions, applied to normally and over consolidated clays, as well as to loose, medium, and dense sand samples. For brevity, only one test is presented here.

The test selected is a saturated drained triaxial test carried out by Been at al. [22] on a sample of a predominantly quartz sand from the Beaufort Sea, North Canada, called Erksak Sand 330/0.7.

The initial void ratio of the sample was $e_0 = 0.59$.

The geometry and the boundary conditions of the simulated test are shown in Fig. 3(a). The sample has a diameter of 7.6 cm and a height of 15.2 cm and was subjected to a constant cell pressure and an axial displacement rate of 5% of the model height per hour.

The input parameters are reported in Table 1.

Table 1. Parameters of the U-CASM used in the saturated simulation.

λ (-)	κ (-)	r (-)	n (-)	M (-)	ν (-)	Γ (-)
0.0135	0.005	6792	4	1.2	0.3	1.82

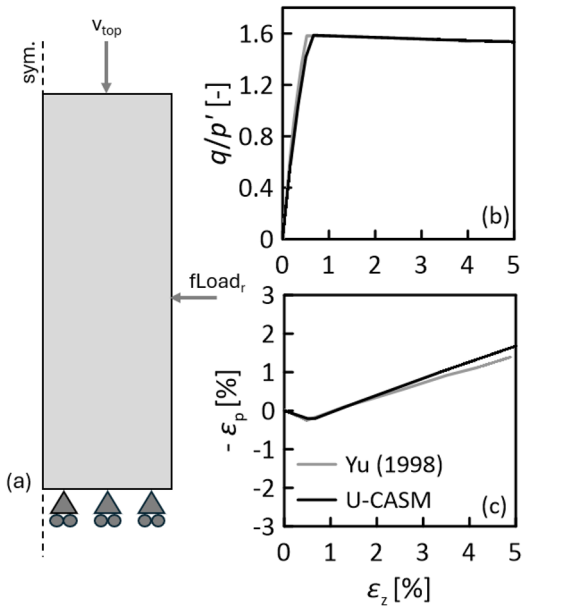

Fig. 3. Drained triaxial test on saturated Erksak Sand 330/0.7, for a dense sample with an initial void ratio $e_0 = 0.59$.

Fig.3.(b) and3.(c) present the simulation results for the stress ratio q/p' versus vertical strain ε_z , and volumetric strain ε_p versus vertical strain ε_z planes , respectively.

Results from the U-CASM are shown as a continuous black line, while those from the implementation proposed in [7] are shown as a grey continuous line.

The two implementations produce results that are in good agreement and the difference are negligible.

4.2 Unsaturated performance of the U-CASM

To evaluate the performance of the U-CASM under partially saturated conditions, a series of simulations were performed to reproduce some triaxial tests on a low plasticity silty sand typical of the Ruedlingen town area, in North-East Switzerland, the Ruedlingen sand. [23].

The numerical results were then compared with those presented by Sitarenios et al. [9] for the same tests.

For brevity, only one of the several unsaturated tests performed on Ruedlingen sand samples is presented in this paper.

The test was conducted on a sample with an initial void ratio of $e_0 = 0.97$ and at a constant water content of $w = 0.25\%$. The sample was subjected to a non-conventional triaxial stress path comprising an initial phase of anisotropic compression at a constant stress ratio equal to $\eta = 0.75$, followed by a reduction in Bishop's effective stress p' while maintaining a constant deviatoric stress q. This type of stress path is particularly relevant for modelling infiltration processes in slopes.

The test was then numerically reproduced, using a water retention curve in the Van Genuchten formulation [17], in which the air entry value was based on porosity, as proposed by Sitarenios et al. [9]:

$$P(n) = P_0 \cdot exp[a(n_0 - n)] \quad (19)$$

where P_0 and n_0 are reference values, and the parameter a governs the rate at which P varies with the porosity n. The saturated permeability was set equal to $K_{sat} = 1 \cdot 10^{-5}$ m/s, while the retention and the mechanical parameters are reported in Table 2 and Table 3, respectively.

Table 2. Hydraulic parameters used in the numerical simulations on the Ruedlingen Sand samples. .

P_0 (kPa)	a (-)	n_0 (-)	$S_{r,max}$ (-)	$S_{r,res}$ (-)	m_{VG} (-)
0.65	21	0.47	1	0.33	0.4

Table 3. Mechanical parameters used in the numerical simulations on the Ruedlingen Sand samples.

λ (-)	κ (-)	r (-)	n (-)	M (-)	ν (-)	Γ (-)
0.0135	0.005	6792	4	1.2	0.3	1.82

Fig. 4.(a) shows the model geometry along with the applied mechanical and hydraulic boundary conditions. The sample was 10 cm high and had a diameter of 5 cm. The magnitude of the applied loads, *fLoadz* and *fLoadr*, is reported in Sitarenios et al. [9].

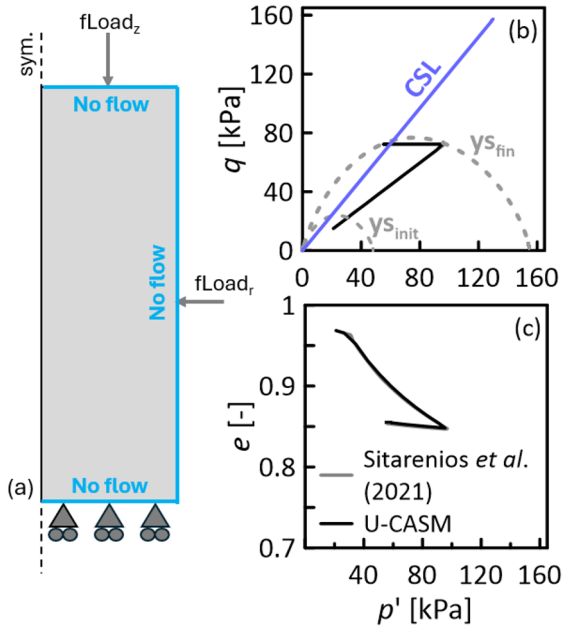

Fig. 4. Unsaturated triaxial test on a Ruedlingen Sand sample, with an initial void ratio $e_0 = 0.97$, at a constant water content of $w = 25\%$, following an unconventional stress path.

Fig. 3.(b) presents the simulation results in terms of stress path, in the Bishop's effective stress, p', versus deviatoric stress, q, plane, while Fig. 3.(c) shows the results in terms of volumetric behaviour in the Bishop's effective stress, p', versus void ratio, e, plane. The grey continuous line represents the results obtained by Sitarenios et al. [9], whereas the solid black line shows the results from the new U-CASM implementation.

As is evident, the two implementations yield the same curves in both planes, thus resulting in identical outcomes.

5 Conclusions

Several constitutive models have been proposed to describe the behaviour of partially saturated soils. Among them, the most widely used is the Barcelona Basic Model (BBM) [1], which adopts suction and net stresses as stress variables. Although this model can effectively capture the behaviour of unsaturated soils, it has some limitations. In particular, the use of net stresses does not allow a natural transition to Terzaghi's effective stresses in saturated conditions and does not directly incorporate the hydraulic behaviour of the soil. As a result, the coupling between mechanical behaviour and the water retention curve, and thus suction changes, is not direct.

To overcome these limitations, this work presents an extension of the *Clay and Sand Model* (CASM), originally formulated for saturated soils, to partially saturated conditions. The extension uses Bishop's effective stress and suction as stress variables. A *loading collapse* surface based on the BBM approach is introduced, together with a Van Genuchten water

retention curve [17], without considering hydraulic hysteresis.

The extended model, referred to as U-CASM, was implemented in COMSOL (2021). Thanks to the symbolic algebra capabilities of the software, all the constitutive functions were written in text format and organised in variable libraries, as described in §3.1. Finally, the model was validated against numerical results from the literature, obtained using the same constitutive model implemented in a different software. The comparisons show a good agreement in both the saturated and partially saturated cases, supporting the reliability of the newly proposed implementation.

The first author acknowledges the PRIN project 'Integrated appPROach for MItigation of flowSlidE risk: full-scale test and advanced numerical modelling' PROMISE. CUP E53D23003430006 for its ongoing financial support and MUR for supporting her scholarship through the PON/DM 1061 (10/08/2021). The second author acknowledges SAFE-LAND Project, funded by EUROPEAN COMMISSION- Directorate-General for European Civil Protection and Humanitarian Aid Operations (ECHO), ECHO.B – Disaster Preparedness and Prevention (Project: 101140345 — SAFE-LAND — UCPM-2023-KAPP).

References

[1].E.E. Alonso, A. Gens, A. Josa, Géotech. **40**, 3, 405–430 (1990)

[2].D.G. Fredlund, H. Rahardjo, Geotech. Spec. Publ., **1**, 1 (1993)

[3].F. M. Francisca, I. Giomi, R. J. Rocca, Comput. Geotech., **167** (2024).

[4].A. Feola, G. Lombardi, A. Pellegrino, C. Viggiani, *Proc. XXII Naz. Conf. Geotech.*, (2004)

[5].A. Gens, Géotech. **60**, 3–74 (2010)

[6].K.H. Roscoe, J.B. Burland, *Eng. Plast., Conf. Papers, Cambridge*, (1968), Univ. Press.

[7].H. S. Yu, Int. J. Numer. Anal. Methods Geomech., **22**, 621–653 (1998)

[8].A. W. Bishop, G. E. Bligh, Geotech., **13**, 177–197 (1963)

[9].P. Sitarenios, F. Casini, A. Askarinejad, S. Springman, Géotech., **71**, 96–109 (2021)

[10]. M. Pirone, G. Vitiello, G. Pedone, F. Casini, A. Santo, G. Urciuoli, *Proc. EUnsat2025* (2025)

[11]. P. W. Rowe, *Proc. R. Soc. Lond. A Math. Phys. Sci.*, **269**, 500–527 (1962)

[12]. A. W. Bishop, Teknisk Ukeblad, **39**, 859–863 (1959)

[13]. J. E. B. Jennings, J. B. Burland, Géotech., **12**, 125–144 (1962)

[14]. B. Loret, N. Khalili, Adv. Numer. Appl. Plast. Geomech., 253–275 (2001)

[15]. N. Lu, J. W. Godt, D. T. Wu, Water Resour. Res., **46**, (2010)

[16]. J. Vaunat, F. Casini, Géotech., **67**, 631–636 (2017)

[17]. M. T. Van Genuchten, Soil Sci. Soc. Am. J., **44**, 892–898 (1980)

[18]. V. Navarro, A. Pucci, E. Tengblad, F. Casini, L. Asensio, Comput. Geotech., **164**, 105834 (2023)

[19]. M. K. Gobbert, A. Churchill, G. Wang, T. I. Seidman, *Proc. COMSOL Conf.*, (2009)

[20]. V. Navarro, L. Asensio, Á. Yustres, X. Pintado, J. Alonso, Eng. Geol., **181**, 190–201 (2014)

[21]. V. Navarro, L. Asensio, H. Gharbieh, G. De la Morena, V. M. Pulkkanen, Nucl. Eng. Technol., **51**, 1047–1059 (2019).

[22]. K. Been, M. G. Jefferies, J. Hachey, Geotech., **41**, 365–381 (1991)

[23]. F. Casini, V. Serri, S. M. Springman, Can. Geotech. *J.*, **50**, 28–40 (2013)